Aggregation behaviors of AB-type brush-*block*-brush amphiphilic copolymers in aqueous media

K. ISHIZU, J. SATOH, K. TOYODA
Department of Organic Materials and Macromolecules, International Research Center of Macromolecular Science, Tokyo Institute of Technology, 2-12-1, Ookayama, Meguro-ku, Tokyo 152-8552, Japan
E-mail: kishizu@polymer.titech.ac.jp

A. SOGABE
Shiseido Research Center, 2-2-1, Hayabuchi, Tsuzuki-ku, Yokohama-city 224-8558, Japan

It is well-known that comb polymers with densely grafted side chains in a good solvent can adopt worm-like cylinder brush conformations, in which the side chains are stretched in the direction normal to the backbone, owing to the excluded-volume interaction. The polymerization of macromonomers provides regular multibranched polymers with dense branching. Since both the degree of polymerization (DP_n) and the length of branches are varied, poly(macromonomer)s, often so-called "polymer brushes," are interesting models for the study of branched polymers [1–9]. More recently, we systematically investigated the architecture of multicomponent copolymer brushes. Fig. 1 shows the illustration of three types of multicomponent copolymer brushes. We have reported the synthesis and dilute-solution properties of poly(diblock macromonomer)s (double-cylinder-type copolymer brushes, see Fig. 1a) by free-radical polymerization of the corresponding diblock macromonomers [10–13]. We also prepared double-cylinder-type copolymer brushes by anionic one-shot polymerization of AB-type diblock nacromonomers [14]. Recently, Matyjaszewski [15] and Müller [16] have also synthesized double-cylinder-type copolymer brushes by the "grafting from" approach, using atom transfer radical polymerization (ATRP). The molecular wires, which are electronic nanodevices, were prepared by forming a linear array of the gold clusters [17] or conducting polypyrroles [18] with an internal core of the double-cylinder-type brushes as templates, whereas the outer cylinder parts work as an insulator.

Ishizu and coworkers established a novel synthesis of prototype amphiphilic copolymer brushes (see Fig. 1b) by alternating free-radical copolymerizations of binary macromonomers [19, 20]. They have also investigated their dilute-solution properties and aggregation behaviors in aqueous media [12, 13, 21, 22]. As a result, such copolymer brushes were molecularly dissolved in a dilute solution and took geometrically anisotropic conformation such as cylinder increasing aspect ratio. In the self-assembly process in water, the hierarchical generation from small rods to large rods, was observed, because such copolymer brushes exhibited phase-separated hydrophobic/hydrophilic domains. Schlüter *et al.* [23] have also synthesized the prototype amphiphilic copolymer brushes by polycondensation of Suzuki-type dendron monomer (hydrophobic/hydrophilic side chains) with dibromic acid ester. More recently, we have reported a novel synthesis of AB-type brush-*block*-brush amphiphilic copolymers (see Fig. 1c) via ATRP [24]. That is, AB-type brush was composed of a polymethacrylate backbone with ester-linked poly(ethylene glycol methylether) (PEG) chains and a polymethacrylate backbone with ester-linked poly(2-hydroxyethyl methacrylate) (PHEMA) side chains. Qin *et al.* [25] also reported such block copolymer brushes via ATRP route. In this paper, we mention the dilute-solution properties of PEG-*block*-PHEMA AB-type brushes and their segregation behaviors in an aqueous medium.

The synthesis route for AB-type brush-*block*-brush amphiphilic copolymers is outlined in Scheme 1. PEG brush macroinitiators (**2**) were prepared by ATRP operations of methacryloyl-terminated PEG macromonomer (PEG-MC; **1**: $M_n = 2000$, $M_w/M_n = 1.19$) initiated by methyl 2-bromopropionate in water under the presence of CuCl and bipyridine (Bpy). CuCl was used as a catalyst with methyl 2-bromopropionate as the initiator. Due to the halogen exchange equilibrium and the relative strengths of the carbon-halogen bonds, the majority of the polymer chains should in fact contain Cl end groups. Characteristics of PEG brush macroinitiators were quoted from Ref. [24] (see Table I). The values of the weight-average molecular weight (M_w) of brush macroinitiators were derived from a Zimm plot by means of static light scattering (SLS; He-Ne laser $\lambda_0 = 632.8$ nm) in benzene at 25 °C. The refractive index increment $[(dn/dc)_{PEG} = -0.034$ (ml/g)] of PEG was used in benzene [8]. The molecular weight distributions (M_w/M_n) were determined by gel permeation chromatography equipped with a low-angle laser light scattering detector (GPC-LALLS; He-Ne laser with a detection angle of 5°) using *N*, *N*-dimethylformamide (DMF)/0.1 M LiBr as the eluant at 40 °C.

PEG brush-*block*-PHEMA block copolymers (**3**) were prepared by the ATRP technique of PEG brush **2** with HEMA in a mixture of methanol/water (1/1 v/v) using the same catalysis system. The degree of PHEMA blocks ($DP_{n,PHEMA}$) was in the range 30–35. Subsequently, the esterification of hydroxy groups (OH) in PHEMA blocks was carried out with

0022–2461

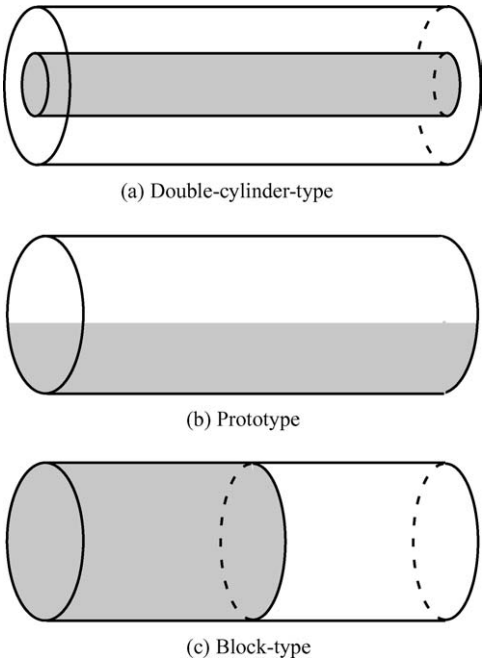

Figure 1 Illustration of multicomponent copolymer brushes.

TABLE I Characteristics of PEG brush macroinitiators

Expt. no.	$10^{-5}\ M_w^a$	M_w/M_n^b	$DP_{n,PMMA}$[c]
B1F	1.38	1.73	40
B3F	0.74	1.86	20
B4F	1.96	1.45	68

[a]Determined by SLS in benzene at 25 °C.
[b]Determined by GPC-LALLS in DMF as eluent.
[c]Degree of polymerization of PMMA backbone calculated from M_n.

TABLE II Characteristics and solution properties of AB-type PEG brush-*block*-PHEMA brush copolymer

Expt. no.	$10^{-5}M_w^a$	M_w/M_n^b	DP_n of PHEMA side chain[c]	$10^7 D_0^d$ (cm^2/s)	R_h^d (nm)	R_g^e (nm)	$R_{g,c}^e$ (nm)
BB1F	2.17	1.78	21	7.4	5.4	7.5	3.9

[a]Determined by SLS in chloroform at 25 °C.
[b]Determined by GPC-LALLS in DMF as eluent at 40 °C.
[c]Calculated from both M_n of copolymer brush and polyinitiator precursor.
[d]Determined by DLS in chloroform at 25 °C.
[e]Determined by SAXS in chloroform using Guinier's plots.

2-bromoisobutyryl bromide (BIB) in 50 wt% tetrahydrofuran (THF) solution, varying the feed ratio of [BIB]/[OH]. This esterification proceeded quantitatively under the large excess amounts of BIB to OH groups. PEG brush-*block*-PHEMA AB-type copolymers (**5**) were prepared by "grafting from" approach using ATRP of polyinitiator (**4**) with HEMA in the mixture of methanol/water. The polymerization systems for polyinitiators with initiation site Br at each pendant end (100% esterification of OH groups in PHEMA blocks) showed heterogeneity due to less solubility of PHEMA. So, AB-type copolymer brush was synthesized using polyinitiator BI1 [starting PEG brush-*block*-PHEMA B1F: P[$(EG)_{40}$-*block*-$(HEMA)_{30}$], number of initiation sites per PHEMA block (N_{BIB}) = 14]. The characteristics of AB-type copolymer brush BB1F were also quoted from Ref. [24] as shown in Table II. The value

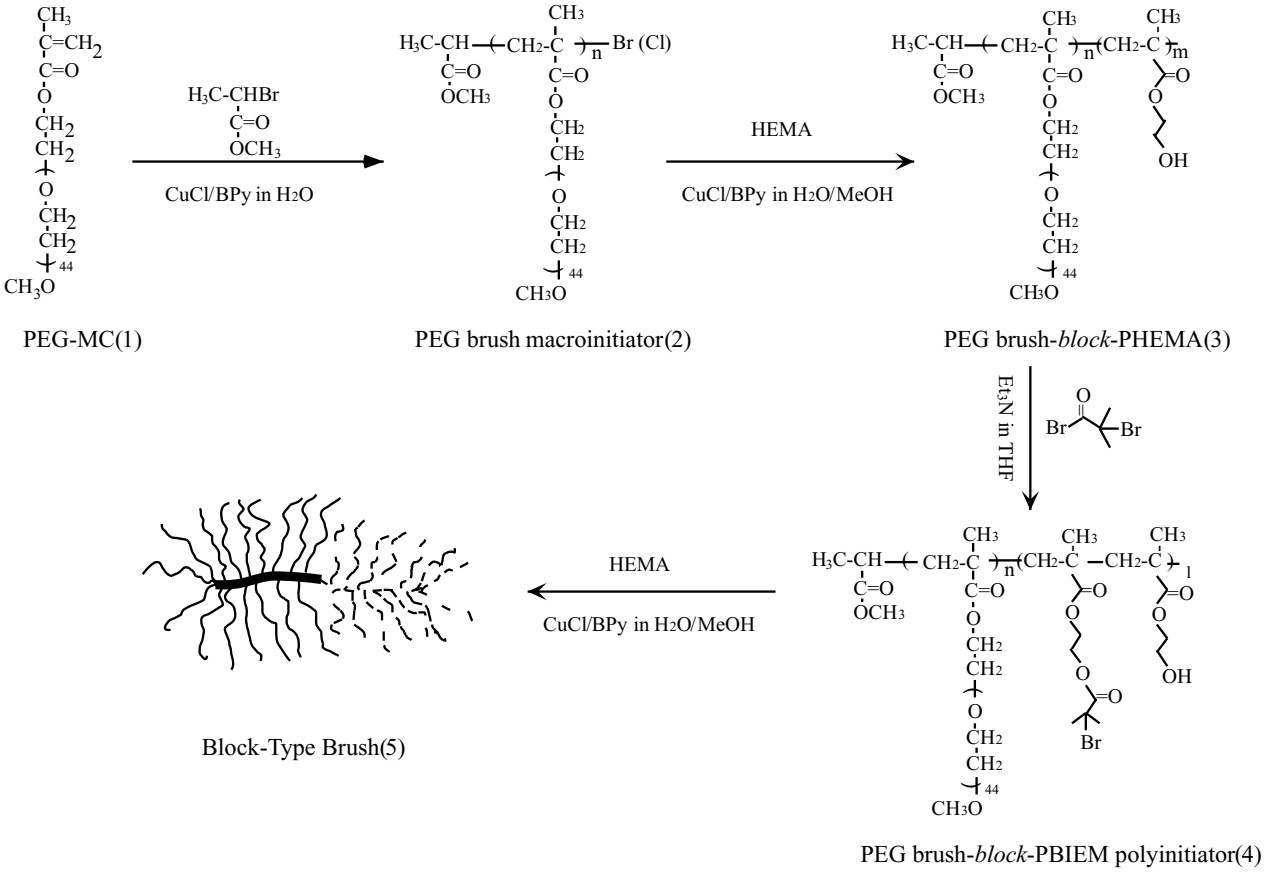

Scheme 1 Reaction scheme for synthesis of AB-type copolymer brushes.

of M_w was derived from a Zimm plot by means of SLS in chloroform at 25 °C. The refractive index increment $[(dn/dc)_{AB}]$ of AB-type brushes was determined by applying the well-known equation

$$(dn/dc)_{AB} = w_{PEG}(dn/dc)_{PEG} + (1 - w_{PEG})(dn/dc)_{PHEMA} \quad (1)$$

where w_{PEG} is the weight fraction of PEG and $(dn/dc)_{PHEMA}$ is the refractive index increment of PHEMA. The values $(dn/dc)_{PEG} = -0.025$ and $(dn/dc)_{PHEMA} = 0.045$ (ml/g) were used in chloroform [26]. This sample BB1F has in total only 70 main chain units ($DP_{n,PMMA} + DP_{n,PHEMA}$) as compared to 45 (PEG) and 21 (PHEMA) side chain units, respectively.

To discuss the geometrical anisotropy and intermolecular interaction, we determined the translational diffusion coefficient (D_0) of polymer brushes by means of dynamic light scattering (DLS) data with negative non-restriction least square (NNLS) method in $CHCl_3$ at 25 °C. The NNLS method is a preferable way of treating the data for polydisperse samples. In general, the mutual diffusion coefficient $D(C)$ is defined as $D(C) \equiv \Gamma_e q^{-2}_{\theta \to 0}$, where θ is the scattering angle. Angular dependences of $\Gamma_e q^{-2}$ ($qR_h < 1$, where R_h is the hydrodynamic radius) for PEG brushes B3F and B4F, and AB-type copolymer brush BB1F are shown in Fig. 2. Polymer concentrations were in the range 4–15 mg/ml benzene solution of PEG brushes and 9–15 mg/ml $CHCl_3$ solution of AB-type copolymer brush, respectively. It is found that the observed data on PEG brush B3F are fitted on an almost flat line. The weak dependence of $\Gamma_e q^{-2}$ on q^2 shows that there is only a single diffusion mode. This brush is composed of a short backbone ($DP_{n,PMMA} = 20$). In general, polymer brushes composed of low DP_n took a star-like conformation in a good solvent [5, 9]. It seems, therefore, that the B3F takes a spherical shape in the dilute solution. On the other hand, PEG brush B4F and copolymer brush BB1F show angular dependence. The PEG brush B4F has in total only 68 (PMMA) main chain units compared to 45 (PEG) side chain units. Therefore, these brush samples seem to take an anisotropic conformation in a dilute solution.

Fig. 3 shows the relationship between translational diffusion coefficient $D(C)$ and polymer concentration for PEG brushes B3F and B4F, and AB-type copolymer brush BB1F. Each $D(C)$ has an almost constant value in the range 4–15 mg/ml of polymer concentration. This suggests that these polymer brushes are molecularly

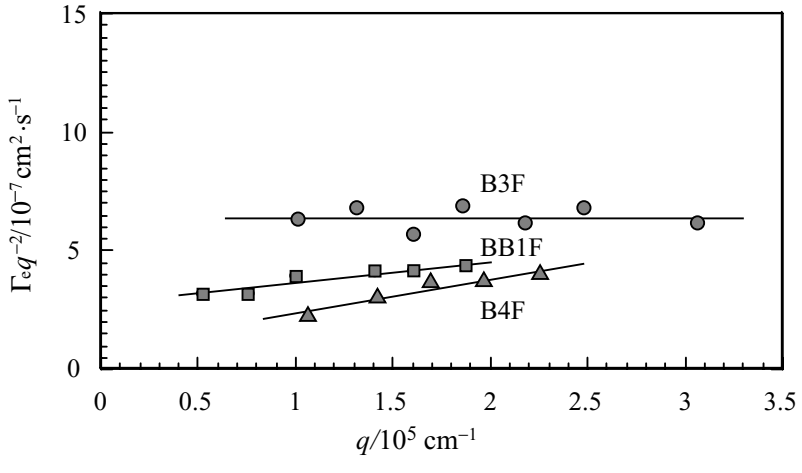

Figure 2 Angular dependence $\Gamma_e q^{-2}$ vs. q^2 for PEG brushes B3F and B4F in benzene, and AB-type copolymer brush BB1F in chloroform.

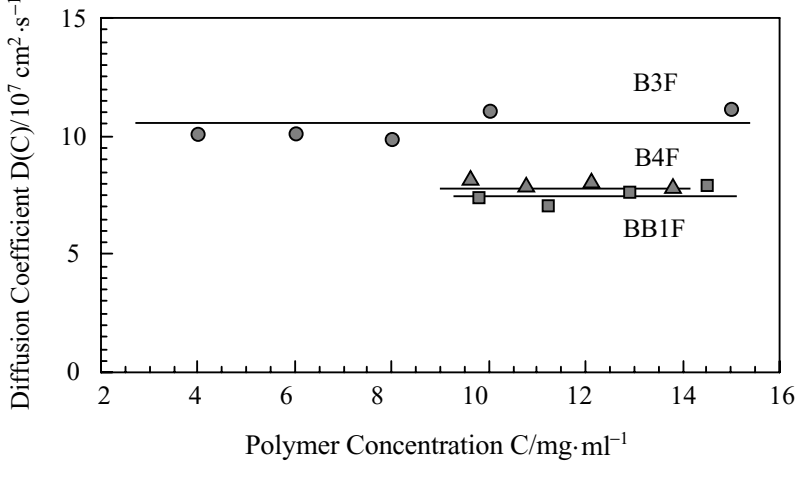

Figure 3 Plots of diffusion coefficient against polymer concentration for PEG brushes B3F and B4F in benzene, and AB-type copolymer brush BB1F in chloroform.

dissolved in the dilute solution. Similar tendencies were also observed in double-cylinder-type [10–13] and prototype [21, 22] copolymer brushes. The translational diffusion coefficient D_0 can be estimated by extrapolation of polymer concentration C to zero. The values of D_0 and R_h for AB-type copolymer brush BB1F are also listed in Table II. R_h is defined as Stokes-Einstein's equation: $R_h = kT/6\pi\eta_0 D_0$, where k, T, and η_0 indicate Boltzmann coefficient, absolute temperature, and viscosity of solvent, respectively. On the other hand, the values of D_0 and R_h for PEG brushes were as follows: B3F; $D_0 = 10.3\times10^{-7}$ cm^2/s, $R_h = 3.5$ nm and B4F; $D_0 = 7.8\times10^{-7}$ cm^2/s, $R_h = 4.6$ nm. D_0 decreased by increasing the molecular weight of polymer brushes.

Since the radius of gyration (R_g) of polymer brushes is very small, it is impossible to evaluate them from SLS. Then, R_g was determined by small-angle X-ray scattering [SAXS; Cu K_α ($\lambda = 1.54$ Å)] in $CHCl_3$. In the measurement of $CHCl_3$ solution (0.5–5.0 wt%) of the AB-type copolymer brush, we used the cell sandwiched between mica plates as a holder vessel. The background correction was carried out using polyethylene film. The value of R_g is estimated by Guinier's method from the following equation [27]:

$$\ln I(q) = \text{const} - (1/3)\left(R_g^2\right)q^2 \tag{2}$$

where q is the scattering vector. The value of cross-sectional radius of gyration ($R_{g,c}$) is estimated from the following equation [28]:

$$\ln[I(q)q] = \text{const} - (1/2)\left(R_{g,c}^2\right)q^2 \tag{3}$$

The values of R_g and $R_{g,c}$ of copolymer brush BB1F were estimated from the corresponding slope of Guinier's plots at the small-angle region ($qR < 1$) (see Fig. 4a and b). These physical values are also listed in Table II. The R_g/R_h value (calculated as 1.4 from Table IV) of BB1F indicates a relatively compact shape.

Assuming a polydispersed rodlike shape (BB1F; $M_w/M_n = 1.78$) and neglecting the cross-sectional dimension, R_g is given by the following relation

$$R_g = L_w/2 \quad \text{for Schulz-Flory length distribution } (L_w/L_n = 2) \tag{4}$$

where L_w denotes the length of a rodlike molecule, Equation 4 allows evaluating the rod length as $L_w =$ 15 nm. The cross-sectional diameter d is calculated from the cross-sectional radius of gyration as

$$d = (\sqrt{8})R_{g,c} \tag{5}$$

by assuming a constant electron density across the cylinder. Since Equation 5 yields $d = 11$ nm, the aspect ratio $L_w/d(1.36)$ of AB-type brush BB1F is not so long. Accordingly, the prepared AB-type sample is more similar to *Janus*-type micelles [29] as sketched in Fig. 5.

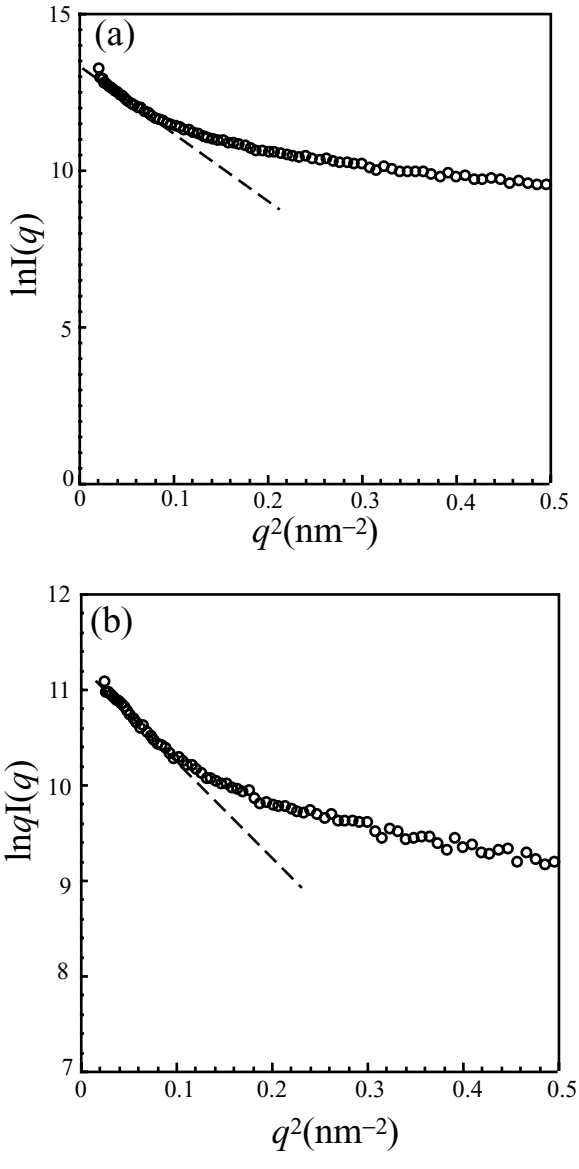

Figure 4 Guinier's plot (a) and cross-sectional Guinier's plot of AB-type copolymer brush BB1F on SAXS in chloroform.

We studied the aggregation behavior of such a *Janus*-type amphiphilic copolymer brush BB1F in an aqueous solution. Fig. 6a shows the hydrodynamic diameter (D_h) distribution of BB1F in an aqueous solution (2×10^{-2} mg/ml) by DLS measurement. Polymer solution showed turbidity but we have never observed the precipitates. An aqueous solution of PEG brushes was homogeneous at the same polymer concentration. Water is a good solvent for PEG but somewhat poor for PHEMA. Single peak is observed at 200 nm. This peak appearing at the larger D_h suggests the presence of aggregates in the system. Fig. 6b shows a typical field emission gun scanning electron microscopy (FE-SEM) photograph of the aggregation product of BB1F (3×10^{-3} mg/ml of aqueous solution was placed onto a glass plate and spin coating was conduced immediately at 3000 rpm for 5 min). The texture shows the existence of large particles (observed diameter; ca. 190 nm). Fig. 7 shows the polymer concentration dependence on the aggregate formation for BB1F. This copolymer brush forms uniform aggregates beyond 10^{-3} until 0.6 mg/ml. However, these aggregates

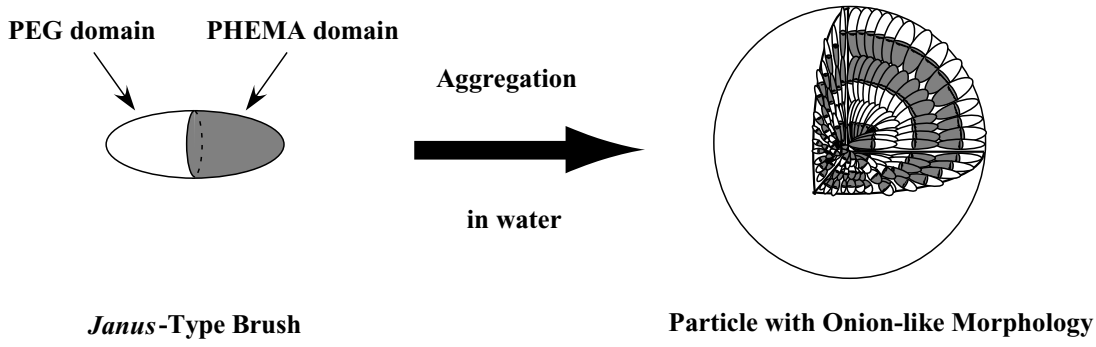

Figure 5 Illustration in aggregation process of *Janus*-type copolymer brushes.

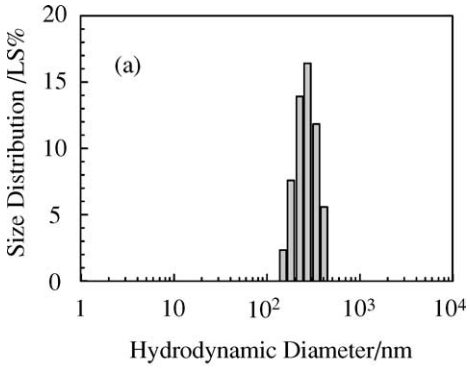

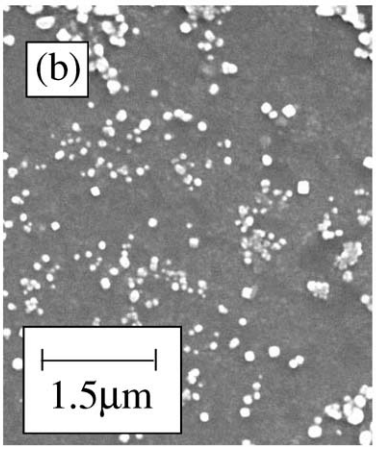

Figure 6 Hydrodynamic diameter distribution of BB1F in water (2×10^{-2} mg/ml) (a) and FE-SEM photograph of BB1F (prepared from 3×10^{-3} mg/ml aqueous solution) (b).

precipitated beyond 0.6 mg/ml. A *Janus*-type ellipsoid of a length 15 nm formed a spherical aggregate of a diameter 200 nm. The aggregation mechanism can be speculated as follows: Less hydrophilic PHEMA domains lead to aggregation with each other in an aqueous solution, and PHEMA core-PEG shell type spherical particles may be formed in the first stage. Subsequently, such PEG shells lead to fusion with PEG domains of *Janus*-type brushes. By repeating these aggregation processes, large multiple-phase particles having "onion-like" morphology (supermicelle) are formed as sketched in Fig. 5. These uniform particles (diameter 200 nm) are stabilized sterically by densely grafted PEG chains in the range 10^{-3}–0.6 mg/ml of polymer concentration.

As mentioned in the introduction, hierarchical generation from small rods to large rods was observed in the self-assembly process of prototype copolymer brushes.

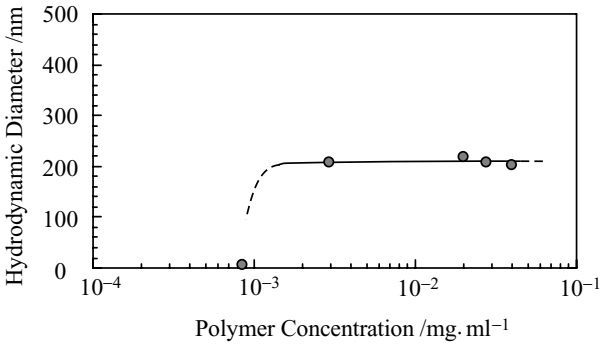

Figure 7 Polymer concentration dependence on the aggregate formation for BB1F in water.

Thus, the trend of an aggregation behavior for *Janus*-type copolymer brushes is very different from that for prototype copolymer brushes. We will investigate the segregation behaviors of AB-type brush-*block*-brush amphiphilic copolymers with various aspect ratios. The results obtained will be reported in the near future.

References

1. M. WINTERMANTEL, K. FISCHER, M. GERLE, R. RIES, M. SCHMIDT, K. KAJIWARA, H. URAKAWA and I. WATAOKA, *Angew. Chem. Int. Eng.* **34** (1995) 1606.
2. M. WINTERMANTEL, M. GERLE, K. FISCHER, M. SCHMIDT, I. WATAOKA, H. URAKAWA, K. KAJIWARA and Y. TSUKAHARA, *Macromolecules* **29** (1996) 978.
3. M. WINTERMANTEL, M. SCHMIDT, Y. TSUKAHARA, K. KAJIWARA and S. KOHJIYA, *Macromol. Rapid Commun.* **15** (1994) 279.
4. Y. TSUKAHARA, S. KOHJIYA, Y. TSUTSUMI and Y. OKAMOTO, *Macromolecules* **27** (1994) 1662.
5. N. NEMOTO, M. NAGAI, A. KOIKE and Y. OKADA, *ibid.* **28** (1995) 3854.
6. I. WATAOKA, H. URAKAWA, K. KAJIWARA, M. SCHMIDT and M. WINTERMANTEL, *Polym. Int.* **44** (1997) 365.
7. K. TERAO, Y. NAKAMURA and T. NORISUYE, *Macromolecular* **32** (1999) 711.
8. S. KAWAGUCHI, G. IMAI, J. SUZUKI, A. MIYAHARA, T. KITANO and K. ITO, *Polymer* **38** (1997) 2885.
9. S. KAWAGUCHI, H. MATSUMOTO, H. IRIANY and K. ITO, *Polym. Prepr. Jpn.* **47** (1998) 1694.
10. K. ISHIZU, K. TSUBAKI and T. ONO, *Polymer* **39** (1998) 2935.
11. K. TSUBAKI and K. ISHIZU, *ibid.* **42** (2001) 8387.
12. K. ISHIZU, K. TSUBAKI, J. SATOH and S. UCHIDA, *Design. Monom. Polym.* **5** (2002) 23.

13. K. ISHIZU, K. TSUBAKI, A. MORI and S. UCHIDA, *Prog. Polym. Sci.* **28** (2003) 27.
14. K. ISHIZU, K. SHIMOMURA, R. SAITO and T. FUKUTOMI, *J Polym. Sci., Polym. Chem. Ed.* **29** (1991) 607.
15. H. G. BORNER, K. BEERS, K. MATYJASZEWSKI, S. S. SHEIKO and M. MÖHLLER, *Macromolecules* **34** (2001) 4375.
16. G. CHENG, A. BOKER, M. ZHANG, G. KRAUSH and A. H. E. MŰLLER, *ibid.* **34** (2001) 6883.
17. R. DJALALI, S.-Y. LI and M. SCHMIDT, *ibid.* **35** (2002) 4282.
18. K. ISHIZU, K. TSUBAKI and S. UCHIDA, *ibid.* **35** (2002) 10193.
19. K. ISHIZU and X. X. SHEN, *Polymer* **40** (1999) 3251.
20. K. ISHIZU, X. X. SHEN and K. TSUBAKI, *ibid.* **41** (2000) 2053.
21. K. TSUBAKI, H. KOBAYASHI, J. SATOH and K. ISHIZU, *J. Colloid Interf. Sci.* **241** (2001) 275.
22. K. ISHIZU, J. SATOH AND K. TSUBAKI, *J. Mater. Sci. Lett.* **20** (2001) 2253.
23. Z. BO, J. P. RABE and A. D. SCHLŰTER, *Angew. Chem. Int. Ed.* **38** (1999) 2370.
24. K. ISHIZU, J. SATOH, K. TOYODA and A. SOGABE, *J. Colloid Interf. Sci.* in press.
25. S. QIN, K. MATYJASZEWSKI, H. XU and S. S. SHEIKO, *Macromolecules* **36** (2003) 605.
26. J. BRANDRUP, E. H. IMMERGUT and E. A. GRULKE, (eds.), in "Polymer Handbook" 4^{th} ed. (John Wiley, New York, 1999).
27. A. GUINIER, *Ann. Phys.* **12** (1939) 161.
28. A. GUINIER and G. FOURNET, "Small-Angle Scattering of X-rays" (John Wiley, New York, 1955).
29. A. MUELLER and D. F. O'BRIEN, *Chem. Rev.* **102** (2002) 727.

Received 5 January
and accepted 10 February 2004